

Dissecting the impact of N-acetylmannosamine (ManNAc) on ganglioside levels in a sialin-deficient cell model

Marya S. Sabir^{1,2}, Marjan Huizing¹, William A. Gahl¹, Frances M. Platt^{3§}, May Christine V. Malicdan^{1§}

¹National Human Genome Research Institute, National Institutes of Health, Bethesda, MD, USA

²NIH Oxford-Cambridge Scholars Program, University of Oxford, Oxford, UK

³Department of Pharmacology, University of Oxford, Oxford, UK

[§]To whom correspondence should be addressed: frances.platt@pharm.ox.ac.uk; maychristine.malicdan@nih.gov

Abstract

Lysosomal free sialic acid storage disorder (FSASD) is an ultra-rare neurodegenerative condition caused by mutations in *SLC17A5*, which encodes the lysosomal sialic acid exporter, sialin. Deficiency of sialin leads to lysosomal accumulation of unconjugated (“free”) sialic acid. This study investigated the ability of N-acetylmannosamine (ManNAc), a precursor of sialic acid, to rescue glycosphingolipid (GSL) sialylation in a *SLC17A5*-deficient HEK-293T model system. Our findings reveal that while ManNAc supplementation may enhance sialic acid biosynthesis, it does not fully restore ganglioside sialylation to wild-type levels, highlighting the essential role of lysosomal sialic acid recycling in maintaining GSL sialylation homeostasis.

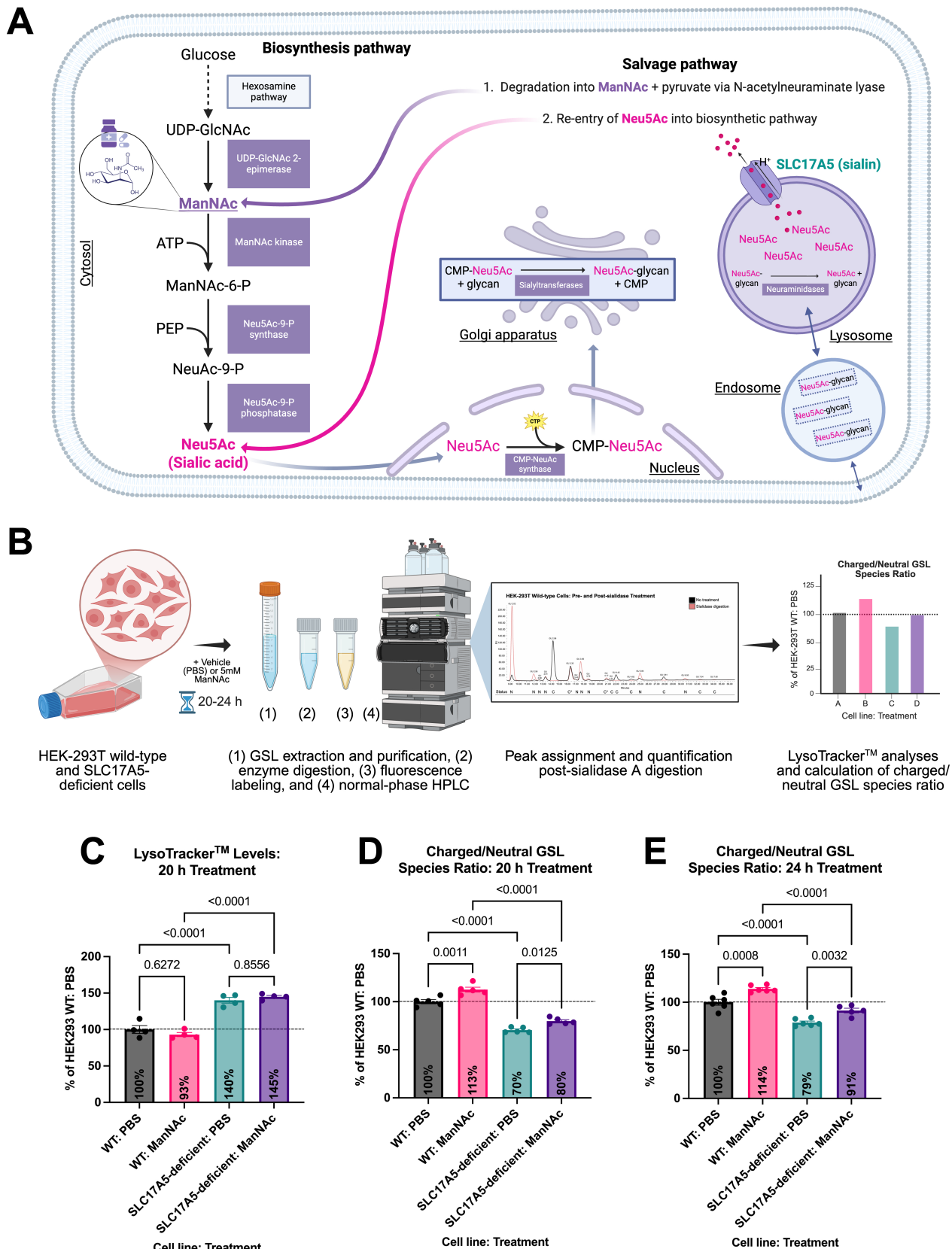


Figure 1. Effects of N-acetylmannosamine (ManNAc) supplementation on lysosomal volume and glycosphingolipid (GSL) profiles in SLC17A5-deficient HEK-293T cells:

(A) Schematic overview of sialic acid biosynthesis and salvage pathways, highlighting the role of ManNAc in the biosynthetic pathway. ManNAc, the only neutral intermediate in the sialic acid biosynthesis pathway, is thought to enter cells via passive diffusion or a plasma membrane transporter, as shown in in vitro systems (Bardor et al., 2005; Hirschberg et al., 1976; Jones et al., 2004). Glycan denotes glycolipids/glycoproteins. Created with BioRender.com. (B) Experimental

workflow for GSL analysis: (1) extraction and purification, (2) enzymatic digestion, (3) fluorescent labeling, and (4) normal-phase HPLC. A 2-AA-labeled glucose homopolymer ladder was used to assign glucose unit (GU) values, and a 2-AA-labeled BioQuant chitotriose standard was used for glycan quantification. Labeled glycans released from GSLs were digested for 16 hours at 37°C with sialidase A. Following digestion, glycans were separated from the enzyme using Microcon-10 filters and analyzed by HPLC. Charged GSL species (labelled “C” on the x-axis) were identified by the disappearance of corresponding peaks after sialidase A digestion, whereas neutral species (labelled “N” on the x-axis) showed no change or increased intensity. Peaks eluting at GU 3.35 and 4.17 likely correspond to GM2 and GM1a, respectively, which persist post-digestion due to internal sialic acid residues, and are considered charged. Quantification was performed by integrating peak areas relative to the chitotriose standard, with GSL abundance normalized to total protein. **(C)** Lysotracker staining-FACS analysis of HEK-293T cells treated with vehicle (PBS) or 5 mM ManNAc for 20 hours (n=4 replicates per genotype-treatment group). **(D)** Quantification of the ratio of charged to neutral GSL species in cells treated for 20 hours, normalized to the PBS-treated HEK-293T wild-type cells. Each group contains n=5-6 replicates per genotype-treatment. **(E)** As in (D), following a 24-hour treatment. Each group contains n=5-6 replicates per genotype-treatment. Data are presented as mean \pm SEM, with statistical significance determined by one-way ANOVA followed by Šidák's multiple comparisons test with *p*-values as indicated.

Description

Lysosomal free sialic acid storage disorder (FSASD) is an ultra-rare, autosomal recessive neurodegenerative disease resulting from pathogenic variants in *SLC17A5* (Adams and Wasserstein, 2020; Verheijen et al., 1999), which encodes the lysosomal membrane transporter, sialin. Sialin mediates the efflux of sialic acid and other acidic hexoses from lysosomes into the cytosol (Blom et al., 1990; Courville et al., 2010; Morin et al., 2004; Pietrancosta et al., 2012). Loss of functional sialin results in lysosomal accumulation of unconjugated (“free”) sialic acid, primarily N-acetylneuraminic acid (Neu5Ac), the most abundant sialic acid in mammals (Schauer, 2009; Varki, 1992). FSASD comprises three main clinical subtypes: infantile FSASD (MIM#269920), an intermediate severe form, and attenuated FSASD (MIM#604369), also referred to as Salla disease, which is typically associated with homozygosity for the common founder variant, p.Arg39Cys (Adams and Wasserstein, 2020; Huizing et al., 2021). Approximately 250 cases have been identified globally, with an estimated 75% of affected individuals carrying the Finnish founder missense variant *SLC17A5* c.115C>T (p.Arg39Cys) in homozygous or compound heterozygous state (Aula et al., 2000; Barmherzig et al., 2017; Huizing et al., 2021). Genotype-phenotype correlations have been described in several studies (Adams and Wasserstein, 2020; Aula et al., 2000; Kleta et al., 2003; Varho et al., 2000).

To date, cellular models of FSASD have been limited to dermal fibroblasts and peripheral blood leukocytes obtained from affected individuals, which have provided mechanistic insights into pathophysiology of the disorder (Baumkotter et al., 1985; Mancini et al., 1992; Mendla and Cantz, 1984; Pitto et al., 1996). Importantly, studies employing fibroblasts have highlighted disrupted turnover of sialoglycoconjugates, including sialoglycoproteins and gangliosides (i.e., sialylated glycosphingolipids or GSLs) in FSASD cells (Chigorno et al., 1996; Pitto et al., 1996). GSLs, including gangliosides, are vital components of the eukaryotic plasma membrane, playing key roles in cell–cell recognition and interaction, regulation of signal transduction pathways, and modulation of inflammatory responses (Schnaar et al., 2022).

While the primary defect in FSASD, namely lysosomal accumulation of free sialic acid is well established, the downstream extra-lysosomal consequences of disrupted sialic acid efflux and its potential impact on sialic acid availability for glycoconjugate sialylation remain poorly understood. The sialin-mediated salvage pathway is presumed to supplement cytoplasmic sialic acid pools used for activation to CMP-Neu5Ac and subsequent incorporation into nascent glycans. However, the relative contribution of this route to steady-state sialylation, particularly in metabolically active or differentiated cells, has not been rigorously quantified. In this study, we utilized a *SLC17A5*-deficient HEK-293T cell model, generated via CRISPR-Cas9-genome editing, to: (1) assess the relative abundance of GlcCer-derived gangliosides (charged) and asialo-GSL (neutral) in the presence of sialin deficiency; and (2) investigate whether supplementation with N-acetylmannosamine (ManNAc), a metabolic precursor of sialic acid, can affect GSL sialylation in the absence of salvage. Given that sialin deficiency disrupts the export of free sialic acid from lysosomes, thereby theoretically reducing its cytoplasmic availability for activation to CMP-sialic acid and subsequent incorporation into sialylated glycoconjugates, we hypothesized that exogenous supplementation with ManNAc—an upstream precursor in the *de novo* sialic acid biosynthetic pathway (**Fig. 1A**)—could enhance cytoplasmic sialic acid levels and thereby improve ganglioside sialylation.

ManNAc has been explored as a therapeutic candidate for GNE myopathy (MIM#605820; NCT04231266), a rare adult-onset neuromuscular disorder (Carrillo et al., 2020). This condition is caused by mutations in the *GNE* gene, which encodes the bifunctional enzyme UDP-N-acetylglucosamine 2-epimerase/ManNAc kinase—the rate-limiting enzyme in sialic acid biosynthesis and a key regulator of cell surface sialylation (Keppler et al., 1999). In GNE mouse models, oral supplementation with ManNAc was shown to improve tissue hyposialylation phenotypes (Malicdan et al., 2009; Niethamer et al., 2012). Supplemental ManNAc, a neutral monosaccharide and the first committed precursor in the sialic

acid biosynthetic pathway, can circumvent feedback inhibition by bypassing the rate-limiting enzymatic step catalyzed by UDP-N-acetylglucosamine 2-epimerase (**Fig. 1A**).

In this study, we treated HEK-293T wild-type and SLC17A5-deficient cells with either phosphate-buffered saline (PBS) as a vehicle control or 5 mM ManNAc for 20 or 24 hours and subsequently analyzed lysosomal volume using LysoTracker™ staining and GSL abundance/composition before and after sialidase A digestion via normal-phase HPLC (**Fig. 1B**). Given that ManNAc supplementation increases sialic acid substrate availability (Peters et al., 2023), it may exacerbate lysosomal storage burden in SLC17A5-deficient cells. Therefore, measuring lysosomal volume via LysoTracker™ staining provides a functional readout to evaluate whether ManNAc treatment results in lysosomal expansion.

In wild-type cells, fluorescently labeled glycans released from GSLs were further digested with sialidase A to distinguish between sialylated (charged) and asialo- (neutral) species (**Fig. 1B – HPLC callout panel**). Compared to PBS-treated wild-type cells, PBS-treated SLC17A5-deficient cells displayed a 1.4-fold increase in LysoTracker™ signal intensity ($p < 0.0001$), consistent with lysosomal expansion, while ManNAc treatment did not significantly alter lysosomal volume in either genotype (**Fig. 1C**). GSL profiling revealed a significant reduction in the ratio of charged to neutral species in PBS-treated SLC17A5-deficient cells compared to wild-type controls, with ratios reduced to 0.70 and 0.79 at 20 and 24 hours, respectively ($p < 0.0001$; **Figs. 1D and 1E**). ManNAc supplementation increased the charged-to-neutral GSL ratio in wild-type cells by 1.13- and 1.14-fold at 20 and 24 hours, respectively, and partially rescued this ratio in SLC17A5-deficient cells, elevating it from 0.70 to 0.80 at 20 hours and from 0.79 to 0.91 at 24 hours ($p < 0.0001$; **Figs. 1D and 1E**). Despite this improvement, the charged-to-neutral GSL ratio in ManNAc-treated SLC17A5-deficient cells remained lower than that observed in wild-type cells treated with either PBS or ManNAc (**Figs. 1D and 1E**).

Collectively, our findings suggest that ManNAc supplementation enhances *de novo* sialic acid biosynthesis, as indicated by the increased ratio of charged to neutral GSL species. However, this increase appears insufficient to fully restore GSL sialylation to wild-type levels in the context of sialin deficiency. These results further highlight the intricate interplay between the biosynthetic and salvage pathways of sialic acid metabolism and suggest that sialin-mediated lysosomal export of sialic acid may be necessary for maintaining cytoplasmic sialic acid pools required for GSL sialylation, an essential process with potential downstream consequences for cellular proliferation (Hakomori, 1970; Robbins and Macpherson, 1971), cell cycle regulation (Chatterjee et al., 1975), and differentiation (Varki, 1993). Importantly, our findings demonstrate that alterations in GSL sialylation precede detectable changes in lysosomal volume following ManNAc treatment—at least at 20 hours—suggesting that GSL sialylation may serve as a more sensitive and tractable cellular phenotype for monitoring early responses to this metabolic intervention.

We acknowledge limitations in this study. First, our analyses were limited to two timepoints—20 and 24 hours—following treatment with vehicle or ManNAc. A more comprehensive time course, including earlier timepoints, would allow for finer resolution of the temporal dynamics of ManNAc uptake, metabolic incorporation, and its downstream effects on GSL sialylation. Next, our study was only conducted in HEK-293T cells; further investigation in disease-relevant cell models, such as patient-derived fibroblasts, leukocytes (Sabir et al., 2025b), and iPSC-derived neural cells (Sabir et al., 2025a) as well as FSASD mouse models (Prolo et al., 2009; Sabir et al., 2022; Sabir et al., 2025b; Stroobants et al., 2017) are needed to determine the generalizability of these findings. Moreover, direct quantification of intracellular sialic acid and analysis of glycoprotein sialylation are needed to further investigate the cellular response to ManNAc supplementation. Despite these limitations, this study represents the first investigation of ManNAc as a potential therapeutic compound for disorders linked to sialin deficiency.

Methods

Generation and culturing of HEK-293T SLC17A5-deficient cells

HEK-293T cells were transfected with a plasmid expressing a single guide RNA targeting exon 2 of the *SLC17A5* gene (Harb et al., 2023) and SpCas9 nuclease, followed by nucleofection using the Lonza 4D Nucleofector X-unit. GFP-positive cells were sorted via flow cytometry, isolated, and expanded into monoclonal colonies. Sanger sequencing of the *SLC17A5* exon 2 region identified three clones with biallelic compound heterozygous mutations in *SLC17A5*. Cells were cultured in feeder media containing high-glucose DMEM supplemented with 10% fetal bovine serum, 1% L-glutamine, and 1% penicillin-streptomycin for downstream studies.

LysoTracker™ staining-FACS analysis

HEK-293T wild-type and SLC17A5-deficient cells were seeded at a density of 50,000 cells per T-25 flask ($n=4$ replicates per genotype-treatment group). Cells were incubated overnight at 37°C in 5% CO₂. The following day, cells were treated with either phosphate-buffered saline (PBS; vehicle control) or 5 mM N-acetylmannosamine (ManNAc; dissolved in PBS) in feeder media (as described above). After 20 hours of incubation, cells were processed, and relative lysosomal volume was assessed using the fluorescent probe LysoTracker™-green DND-26 as previously described (te Vruchte et al., 2014). Briefly, cells were harvested and washed twice with PBS, followed by staining with 200 nM LysoTracker™ for 10

minutes in the dark. After staining, cells were washed again with PBS and resuspended in buffer containing 5 µg/ml propidium iodide to exclude non-viable cells. Samples were immediately analyzed on a BD FACS-Canto II flow cytometer (Becton Dickinson). For each sample, a minimum of 10,000 events were acquired using the DIVA software (Becton Dickinson, version *.0.1), and relative fluorescence intensity was quantified using the FlowJo software (FlowJo, LLC; version 10). A representative flow cytometry plot of LysoTracker™ staining in wild-type and SLC17A5-deficient HEK-293T cells is shown in the extended data (HEK_ManNAc flow cytometry plot).

Note, the concentration of 5 mM ManNAc was selected based on prior studies demonstrating that this dose effectively restores polysialylation to near wild-type levels in cultured HEK-293T wild-type and *GNE* knock-out cells (Neu et al., 2024).

Profiling cellular GSLs

HEK-293T wild-type and SLC17A5-deficient cells were plated at a density of 200,000 cells per T-25 flask, with n=5-6 replicates per genotype-treatment group. Cells were treated with either PBS vehicle or 5 mM ManNAc in feeder media (described above). At 20 and 24 hours post-treatment, cells were harvested and lysed in water using three freeze-thaw cycles.

GSL profiling was performed as previously described (Priestman et al., 2024). Briefly, lipids were extracted overnight at 4°C using chloroform:methanol. GSLs were subsequently isolated by solid-phase extraction on C18 columns. Eluted fractions were evaporated under nitrogen at 42 °C, and dried samples were subjected to enzymatic digestion using recombinant ceramide glycanase to release glycans from complex GSLs. Released oligosaccharides were fluorescently labeled with anthranilic acid (2-AA), and excess label was removed using DPA-6S solid-phase extraction columns. Purified 2-AA-labeled glycans were analyzed by normal-phase high-performance liquid chromatography (HPLC). A 2-AA-labeled glucose homopolymer ladder was used to assign glucose unit (GU) values. Glycan quantification was performed by integrating peak areas relative to a 2-AA-labeled BioQuant chitotriose standard. GSL abundance was normalized to total protein content, determined using the bicinchoninic acid (BCA) assay following standard procedures.

Sialidase A digestion and calculation of charged to neutral GSL species ratio

Labeled glycans released from HEK-293T GSLs were digested for 16 hours at 37°C in a total volume of 10 µl with sialidase A according to manufacturer's instructions. Following digestion, labeled glycans were separated from enzyme using Microcon-10 Centrifugal Filters before HPLC as described above.

Charged GSL species were identified by the loss of corresponding peaks following sialidase A digestion, while neutral species exhibited no change or an increase in peak intensity, reflecting the sequential degradation of gangliosides (**Fig. 1B – HPLC callout panel**). Notably, peaks eluting at GU 3.35 and 4.17 likely correspond to GM2 and GM1a, respectively (**Fig. 1B – HPLC callout panel**). These gangliosides contain internal (non-terminal) sialic acid residues, which are not cleaved by sialidase A, explaining the persistence of their peaks post-digestion. Thus, these two peaks are considered to be charged. The charged-to-neutral GSL species ratio was calculated by summing all charged species and dividing by the sum of neutral species, then expressed as a percentage relative to the HEK-293T wild-type PBS reference group.

Statistical analyses

Statistical analyses were conducted using ordinary one-way ANOVA with Šídák's multiple comparisons test using GraphPad Prism (GraphPad, version 10.0.3). A two-tailed α -value for significance was set at 0.05.

Reagents

Reagent	Supplier	Catalog number
DMEM-high glucose	Sigma-Aldrich	D5671
Fetal bovine serum	Sigma-Aldrich	F7524
Penicillin-streptomycin	Sigma-Aldrich	P0781
L-Glutamine (200 mM)	ThermoFisher Scientific	25030024
Phosphate-buffered saline (PBS); no calcium, no magnesium	ThermoFisher Scientific	14190250

Trypsin-EDTA (0.25%), phenol red	ThermoFisher Scientific	25200056
N-acetylmannosamine (ManNAc)	New Zealand Pharmaceuticals	Custom order
LysoTracker™ Green DND-26	ThermoFisher Scientific	L7526
Propidium iodide solution	Millipore Sigma	537060
Ceramide glycanase (rEGCase)	GenScript	Custom order
Kinesis SPE Columns: TELOS® C18(EC) 100mg/1ml SPE Columns	Cole-Parmer	EW-06476-81
Discovery® DPA-6S SPE Tube	Millipore Sigma	52624-U
Anthranilic acid (2-AA)	Sigma-Aldrich	A89855
Glucose homopolymer ladder (2-AA labeled)	Ludger Ltd.	CAA-GHP-30
Ludger-BioQuant chitotriose standard (2-AA labeled)	Ludger Ltd.	BQ-CAA-CHI-01
Bicinchoninic acid solution	Millipore Sigma	B9643-1L
AdvanceBio Sialidase A	Agilent	GK80040
Microcon-10 Centrifugal Filters	Millipore Sigma	MRCPR010

Acknowledgements: We would like to extend our gratitude to Drs. Allisandra K. Rha and Raymond Y. Wang from the Children's Hospital of Orange County for generating and generously sharing the HEK-293T SLC17A5-deficient cell line. We are grateful to Ms. Carla Ciccone (NHGRI/NIH) for her help with shipments. We thank Ms. Dawn Shepherd and Ms. Danielle Taylor-Te Vrugte (University of Oxford) for their expert guidance on the LysoTracker™ and sialidase A experiments, respectively.

Extended Data

Description: HEK_ManNAc flow cytometry plot. Resource Type: Image. File: [HEK_ManNAc_flow_cytometry_plot.pdf](#). DOI: [10.22002/vh16y-vxj14](#)

References

- Adams D, Wasserstein M. 2020. Free Sialic Acid Storage Disorders. GeneReviews((R)) 2. PubMed ID: [20301643](#)
- Aula N, Salomaki P, Timonen R, Verheijen F, Mancini G, Mansson JE, Aula P, Peltonen L. 2000. The spectrum of SLC17A5-gene mutations resulting in free sialic acid-storage diseases indicates some genotype-phenotype correlation. Am J Hum Genet. 67: 832-40. 10. PubMed ID: [10947946](#)
- Bardor M, Nguyen DH, Diaz S, Varki A. 2005. Mechanism of uptake and incorporation of the non-human sialic acid N-glycolylneuraminic acid into human cells. J Biol Chem. 280: 4228-37. 40. PubMed ID: [15557321](#)
- Barmherzig R, Bullivant G, Cordeiro D, Sinasac DS, Blaser S, Mercimek Mahmutoglu S. 2017. A New Patient With Intermediate Severe Salla Disease With Hypomyelination: A Literature Review for Salla Disease. Pediatr Neurol. 74: 87-91 e2. 11. PubMed ID: [28662915](#)
- Baumkötter J, Cantz M, Mendla K, Baumann W, Friebohn H, Gehler J, Spranger J. 1985. N-Acetylneuraminic acid storage disease. Hum Genet. 71: 155-9. 16. PubMed ID: [4043964](#)
- Blom HJ, Andersson HC, Seppala R, Tietze F, Gahl WA. 1990. Defective glucuronic acid transport from lysosomes of infantile free sialic acid storage disease fibroblasts. Biochem J. 268: 621-5. 3. PubMed ID: [2363700](#)
- Carrillo N, Malicdan MC, Huizing M. 2020. GNE Myopathy. GeneReviews((R)) 20. PubMed ID: [20301439](#)

- Chatterjee S, Sweeley CC, Velicer LF. 1975. Glycosphingolipids of human KB cells grown in monolayer, suspension, and synchronized cultures. *J Biol Chem.* 250: 61-6. 27. PubMed ID: [1141212](#)
- Chigorno V, Tettamanti G, Sonnino S. 1996. Metabolic processing of gangliosides by normal and Salla human fibroblasts in culture. A study performed by administering radioactive GM3 ganglioside. *J Biol Chem.* 271: 21738-44. 18. PubMed ID: [8702969](#)
- Courville P, Quick M, Reimer RJ. 2010. Structure-function studies of the SLC17 transporter sialin identify crucial residues and substrate-induced conformational changes. *J Biol Chem.* 285: 19316-23. 4. PubMed ID: [20424173](#)
- Hakomori S. 1970. Cell density-dependent changes of glycolipid concentrations in fibroblasts, and loss of this response in virus-transformed cells. *Proc Natl Acad Sci U S A.* 67: 1741-7. 25. PubMed ID: [4321344](#)
- Harb JF, Christensen CL, Kan SH, Rha AK, Andrade Heckman P, Pollard L, et al., Wang RY. 2023. Base editing corrects the common Salla disease SLC17A5 c.115C>T variant. *Mol Ther Nucleic Acids.* 34: 102022. 34. PubMed ID: [37727271](#)
- Hirschberg CB, Goodman SR, Green C. 1976. Sialic acid uptake by fibroblasts. *Biochemistry.* 15: 3591-9. 38. PubMed ID: [821521](#)
- Huizing M, Hackbarth ME, Adams DR, Wasserstein M, Patterson MC, Walkley SU, Gahl WA, Consortium F. 2021. Free sialic acid storage disorder: Progress and promise. *Neurosci Lett.* 755: 135896. 9. PubMed ID: [33862140](#)
- Jones MB, Teng H, Rhee JK, Lahar N, Baskaran G, Yarema KJ. 2004. Characterization of the cellular uptake and metabolic conversion of acetylated N-acetylmannosamine (ManNAc) analogues to sialic acids. *Biotechnol Bioeng.* 85: 394-405. 39. PubMed ID: [14755557](#)
- Keppler OT, Hinderlich S, Langner J, Schwartz Albiez R, Reutter W, Pawlita M. 1999. UDP-GlcNAc 2-epimerase: a regulator of cell surface sialylation. *Science.* 284: 1372-6. 21. PubMed ID: [10334995](#)
- Kleta R, Aughton DJ, Rivkin MJ, Huizing M, Strovel E, Anikster Y, et al., Gahl WA. 2003. Biochemical and molecular analyses of infantile free sialic acid storage disease in North American children. *Am J Med Genet A.* 120A: 28-33. 12. PubMed ID: [12794688](#)
- Malicdan MC, Noguchi S, Hayashi YK, Nonaka I, Nishino I. 2009. Prophylactic treatment with sialic acid metabolites precludes the development of the myopathic phenotype in the DMRV-hIBM mouse model. *Nat Med.* 15: 690-5. 23. PubMed ID: [19448634](#)
- Mancini GM, Hu P, Verheijen FW, Van Diggelen OP, Janse HC, Kleijer WJ, Beemer FA, Jennekens FG. 1992. Salla disease variant in a Dutch patient. Potential value of polymorphonuclear leucocytes for heterozygote detection. *Eur J Pediatr.* 151: 590-5. 17. PubMed ID: [1505579](#)
- Mendla K, Cantz M. 1984. Specificity studies on the oligosaccharide neuraminidase of human fibroblasts. *Biochem J.* 218: 625-8. 15. PubMed ID: [6424662](#)
- Morin P, Sagne C, Gasnier B. 2004. Functional characterization of wild-type and mutant human sialin. *EMBO J.* 23: 4560-70. 5. PubMed ID: [15510212](#)
- Neu CT, Weilepp L, Bork K, Gesper A, Horstkorte R. 2024. GNE deficiency impairs Myogenesis in C2C12 cells and cannot be rescued by ManNAc supplementation. *Glycobiology.* 34 36. PubMed ID: [38224318](#)
- Niethamer TK, Yardeni T, Leoyklang P, Ciccone C, Astiz Martinez A, Jacobs K, et al., Huizing M. 2012. Oral monosaccharide therapies to reverse renal and muscle hyposialylation in a mouse model of GNE myopathy. *Mol Genet Metab.* 107: 748-55. 22. PubMed ID: [23122659](#)
- Peters E, Selke P, Bork K, Horstkorte R, Gesper A. 2023. Evaluation of N-Acetylmannosamine Administration to Restore Sialylation in GNE-Deficient Human Embryonal Kidney Cells. *Front Biosci (Landmark Ed).* 28: 300. 24. PubMed ID: [38062838](#)
- Pietrancosta N, Anne C, Prescher H, Ruivo R, Sagne C, Debacker C, et al., Gasnier B. 2012. Successful prediction of substrate-binding pocket in SLC17 transporter sialin. *J Biol Chem.* 287: 11489-97. 6. PubMed ID: [22334707](#)
- Pitto M, Chigorno V, Renlund M, Tettamanti G. 1996. Impairment of ganglioside metabolism in cultured fibroblasts from Salla patients. *Clin Chim Acta.* 247: 143-57. 14. PubMed ID: [8920233](#)
- Priestman DA, Weng Y, Sabir MS, Bush R, Te Vruchte D, Wallom K, Fernandez Suarez ME, Platt FM. 2024. Analysis of glycosphingolipids from cell lines. 37. DOI: [dx.doi.org/10.17504/protocols.io.x54v9pn14g3e/v1](https://doi.org/10.17504/protocols.io.x54v9pn14g3e/v1)
- Prolo LM, Vogel H, Reimer RJ. 2009. The lysosomal sialic acid transporter sialin is required for normal CNS myelination. *J Neurosci.* 29: 15355-65. 31. PubMed ID: [20007460](#)
- Robbins PW, Macpherson I. 1971. Control of glycolipid synthesis in a cultured hamster cell line. *Nature.* 229: 569-70. 26. PubMed ID: [4925360](#)

Sabir MS, Hackbarth ME, Burke JD, Garrett LJ, Elliott G, Rivas C, et al., Malicdan MCV. 2022. A novel experimental mouse model to investigate a free sialic acid storage disorder (Salla disease). *Molecular Genetics and Metabolism*. 135: S107. 33. DOI: [10.1016/j.ymgme.2021.11.283](https://doi.org/10.1016/j.ymgme.2021.11.283)

Sabir MS, Jovanovic VM, Ryu S, Sen C, Ormanoglu P, Pollard L, et al., Malicdan MCV. 2025. Lysosomal free sialic acid storage disorder iPSC-derived neural cells display altered glycosphingolipid metabolism. *Sci Rep*. 15: 29708. 30. PubMed ID: [40804080](https://pubmed.ncbi.nlm.nih.gov/40804080/)

Sabir MS, Pollard L, Wolfe L, Adams DR, Ciccone C, Leoyklang P, et al., Malicdan MCV. 2025. Investigating the Utility of Leukocyte Sialic Acid Measurements in Lysosomal Free Sialic Acid Storage Disorder. *JIMD Reports*. 66: e70029. 29. DOI: <https://doi.org/10.1002/jmd2.70029>

Schauer R. 2009. Sialic acids as regulators of molecular and cellular interactions. *Curr Opin Struct Biol*. 19: 507-14. 7. PubMed ID: [19699080](https://pubmed.ncbi.nlm.nih.gov/19699080/)

Schnaar RL, Sandhoff R, Tiemeyer M, Kinoshita T. 2022. Glycosphingolipids. *Essentials of Glycobiology*: 129-40. 19. PubMed ID: [35536927](https://pubmed.ncbi.nlm.nih.gov/35536927/)

Stroobants S, Van Acker NG, Verheijen FW, Goris I, Daneels GF, Schot R, et al., D Hooge R. 2017. Progressive leukoencephalopathy impairs neurobehavioral development in sialin-deficient mice. *Exp Neurol*. 291: 106-119. 32. PubMed ID: [28189729](https://pubmed.ncbi.nlm.nih.gov/28189729/)

Te Vruchte D, Speak AO, Wallom KL, Al Eisa N, Smith DA, Hendriksz CJ, et al., Platt FM. 2014. Relative acidic compartment volume as a lysosomal storage disorder-associated biomarker. *J Clin Invest*. 124: 1320-8. 35. PubMed ID: [24487591](https://pubmed.ncbi.nlm.nih.gov/24487591/)

Varho T, Jaaskelainen S, Tolonen U, Sonninen P, Vainionpaa L, Aula P, Sillanpaa M. 2000. Central and peripheral nervous system dysfunction in the clinical variation of Salla disease. *Neurology*. 55: 99-104. 13. PubMed ID: [10891913](https://pubmed.ncbi.nlm.nih.gov/10891913/)

Varki A. 1992. Diversity in the sialic acids. *Glycobiology*. 2: 25-40. 8. PubMed ID: [1550987](https://pubmed.ncbi.nlm.nih.gov/1550987/)

Varki A. 1993. Biological roles of oligosaccharides: all of the theories are correct. *Glycobiology*. 3: 97-130. 28. PubMed ID: [8490246](https://pubmed.ncbi.nlm.nih.gov/8490246/)

Verheijen FW, Verbeek E, Aula N, Beerens CE, Havelaar AC, Joosse M, et al., Mancini GM. 1999. A new gene, encoding an anion transporter, is mutated in sialic acid storage diseases. *Nat Genet*. 23: 462-5. 1. PubMed ID: [10581036](https://pubmed.ncbi.nlm.nih.gov/10581036/)

Funding: This work was supported in part by the National Institutes of Health (NIH) Intramural Research Program of the National Human Genome Research Institute. The contributions of the NIH authors are considered works of the U.S. Government. The findings and conclusions presented in this paper are those of the authors and do not necessarily reflect the views of the NIH or the U.S. Department of Health and Human Services. MSS received a graduate fellowship from the National Institutes of Health Oxford-Cambridge Scholars Program.

Author Contributions: Marya S. Sabir: conceptualization, investigation, formal analysis, visualization, writing - original draft, writing - review editing. Marjan Huizing: supervision, writing - review editing. William A. Gahl: supervision, funding acquisition, writing - review editing. Frances M. Platt: conceptualization, writing - review editing, supervision, funding acquisition. May Christine V. Malicdan: conceptualization, writing - review editing, supervision.

Reviewed By: Anonymous

History: Received July 2, 2025 **Revision Received** August 27, 2025 **Accepted** September 2, 2025 **Published Online** September 2, 2025 **Indexed** September 16, 2025

Copyright: © 2025 by the authors. This is an open-access article distributed under the terms of the Creative Commons Attribution 4.0 International (CC BY 4.0) License, which permits unrestricted use, distribution, and reproduction in any medium, provided the original author and source are credited.

Citation: Sabir MS, Huizing M, Gahl WA, Platt FM, Malicdan MCV. 2025. Dissecting the impact of N-acetylmannosamine (ManNAc) on ganglioside levels in a sialin-deficient cell model. *microPublication Biology*. [10.17912/micropub.biology.001733](https://doi.org/10.17912/micropub.biology.001733)